9
Beyond mean field

The Hartree–Fock mean field is represented by a static potential. Non-locality may be approximated by a momentum dependence but the potential is energy independent. In general, independent particle motion is renormalized by coupling to more complicated degrees of freedom. Such couplings often involve a time delay and introduce an energy dependence into the single-particle motion. For example the effective interaction of two nucleons mediated by coupling to a surface vibration has an energy dependence related to the frequency of the vibrational mode.

The state of motion of a nucleon in a nucleus may change by a core polarization process where it promotes a nucleon from a state in the Fermi sea to a state above the Fermi surface as illustrated in Fig. 9.1 (see also Fig. 8.3(b)), or by an inelastic collision as illustrated in Fig. 8.10. This is an example of the doorway phenomenon, the states containing a nucleon and a vibration being the doorway states. The original formulation of the concepts of doorway state can be found in Block and Feshbach (1963). The review by Feshbach (1974) contains details of subsequent developments.

9.1 Doorway states

Through the coupling introduced in equation (8.24) a particle can set the nuclear surface into vibration. Such process can be repeated, the particle interacting a second time with the surface and reabsorbing the vibration (see Fig. 9.2). In this way the particle becomes dressed and the properties characterizing the nucleon, such as mass, charge, mean free path, occupation number, etc., are modified due to this coupling.

https://doi.org/10.1017/9781009401920.010 Published online by Cambridge University Press

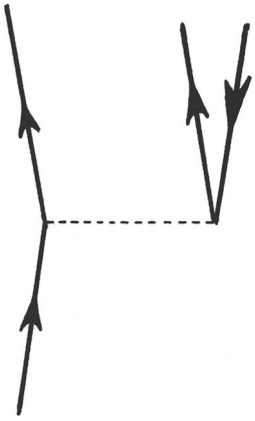

Figure 9.1. Collision between nucleons where a particle changes state of motion by inducing a particle–hole core excitation.

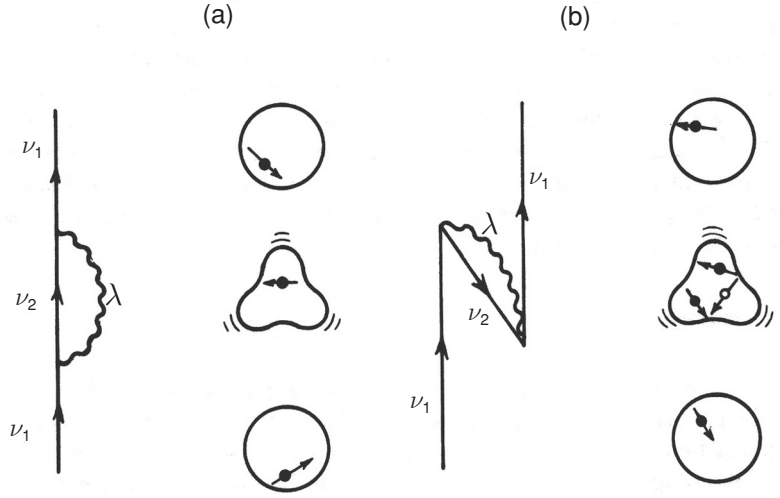

Figure 9.2. The lowest-order process by which the single-particle motion is renormalized by the coupling to the nuclear surface. In (a) the particle excites the vibration by bouncing inelastically off the surface. In (b) the vibration is excited by a virtual process (vacuum fluctuation). Particles are represented by an upwardgoing arrowed line (by a solid dot) while holes are pictured as a downwardgoing arrowed line (open circle). The surface vibration is drawn as a wavy line.

9.1.1 The dynamical shell model

The self-energy Σ of a nucleon in a nucleus is the renormalization of single particle or single hole energies due to coupling of single-particle motion to more complicated degrees of freedom. The present chapter will focus on the

https://doi.org/10.1017/9781009401920.010 Published online by Cambridge University Press

self-energy due to the coupling of single-particle motion to nuclear surface vibrations (the coupling to pairing vibrations in rotating nuclei was discussed in Chapter 6, in particular in Sections 6.3 and 6.4). The relevant processes in lowest order are illustrated in Fig. 9.2. The corresponding perturbation expression of the self-energy operator for a particle state is

$$\Sigma(\nu_1, \omega) = \sum_{\lambda, \varepsilon_2 > \varepsilon_F} \frac{V^2(\nu_1, \nu_2; \lambda)}{\omega - (\varepsilon_2 + \omega_\lambda)} - \sum_{\lambda, \varepsilon_2 < \varepsilon_F} \frac{V^2(\nu_1, \nu_2; \lambda)}{-\omega + (\varepsilon_2 - \omega_\lambda)}, \tag{9.1}$$

where the minus sign in the second term arises because of fermion exchange (Pauli principle). Each term of this expression has the typical structure of an energy correction in second-order perturbation theory, i.e. a square matrix element divided by an energy denominator. In equation (9.1) ω is the energy of the initial single-particle state $|\nu_1\rangle$. The phonons associated with the surface vibrations have energy ω_λ and multipolarity λ. The quantities $V(\nu_1, \nu_2; \lambda)$ are the particle-vibration coupling matrix elements which were defined in equation (8.31). The energy denominators are the energy differences between the initial and the intermediate states. The first term in equation (9.1) corresponds to the polarization graph in Fig. 9.2(a). The energies of both the initial single-particle state and the intermediate particle state ε_2 are both greater than the Fermi energy ε_F. The second term illustrated by the graph in Fig. 9.2(b) is associated with core correlations and the intermediate state $|\nu_2^{-1}\rangle$ is a hole state with energy $\varepsilon_2 < \varepsilon_F$.

Some general conclusions can be drawn from the structure of equation (9.1). The first term is negative for particle states with energies relative to the Fermi energy which are lower than the phonon energy, $\varepsilon_1 - \varepsilon_F < \hbar\omega_\lambda$. There is a cancellation between negative and positive contributions for high-energy single-particle states $\varepsilon_1 - \varepsilon_F \gg \hbar\omega_\lambda$. The second term is always positive because $\varepsilon_1 - \varepsilon_2 > 0$ and $\omega_\lambda > 0$. The net result is that low-energy single-particle states have a negative self-energy and are shifted towards the Fermi level. This shift has a maximum when $\varepsilon_1 - \varepsilon_F \approx \hbar\omega_\lambda$ and decreases or even changes sign for high single-particle states. The self-energy has the opposite sign for hole states and the resulting effect is to narrow the energy gap between particle states and hole states. A number of calculations starting from that of Bertsch and Kuo (1968) support these conclusions (see Mahaux *et al*. (1985) and references therein).

Both terms in equation (9.1) are important for an initial state $|\nu_1\rangle$ near the Fermi level and, in a Fermi gas model, the self-energy $\Sigma(\nu_1) \approx 0$ at the Fermi level due to a cancellation between the two terms. The first term in equation (9.1) is more important for an initial state $|\nu_1\rangle$ away from the Fermi level because the energy denominators are smaller. In the following we will make a simple estimate of the quantity $\Sigma(\nu_1)$ neglecting the second term. The first term can be written

more explicitly as

$$\Sigma(\nu_1) = \sum_{\nu_2,\lambda} \frac{V^2(\nu_1, \nu_2, \lambda)}{\varepsilon_1 - (\varepsilon_2 + \hbar\omega_\lambda)} = \sum_{\nu_2\lambda} \frac{{\beta_\lambda}^2}{(2j_2+1)(2\lambda+1)} \frac{\langle j_2|R_0 \frac{\partial U}{\partial r}|j_1\rangle^2 \langle l_2 j_2||Y_\lambda||l_1 j_1\rangle^2}{\varepsilon_1 - (\varepsilon_2 + \hbar\omega_\lambda)}, \tag{9.2}$$

where the statistical factors and reduced matrix element of the spherical harmonic $Y_{\lambda\mu}$ associated with angular momentum coupling are shown explicitly (see Appendix D). There is a parity constraint and $l_1 + l_2 - \lambda$ is restricted to being even.

When $\nu_2 = \nu_1$ the phonon multipolarity λ must be even because of the parity constraint. Assuming furthermore that $j_1 \gg \lambda$, one can use the asymptotic form of the $3j$-symbols and write (see Appendix D)

$$\langle l_1 j_1||Y_\lambda||l_1 j_1\rangle^2 \approx 0.1(2j_1+1), \quad \text{when } \lambda \text{ is even.} \tag{9.3}$$

The squared matrix element coupling the nucleon with the vibration can then be expressed as

$$V^2(\nu_1, \nu_1; \lambda) = \frac{0.1{\beta_\lambda}^2}{(2\lambda+1)} \langle j_1|R_0 \frac{\partial U}{\partial r}|j_1\rangle^2, \tag{9.4}$$

and the quantity $\Sigma(\nu_1)$ becomes

$$\Sigma(\nu_1) \approx \sum_\lambda \Sigma^\lambda(\nu_1), \tag{9.5}$$

where

$$\Sigma^\lambda(\nu_1, \omega) = -\frac{V^2(\nu_1, \nu_1; \lambda)}{\hbar\omega_\lambda}. \tag{9.6}$$

The numerators of all the factors appearing in the above equations have a similar magnitude for both low-lying collective surface vibrations and for high-lying modes. Because the energy $\hbar\omega_\lambda$ is much smaller for low-lying modes than for giant resonances, we shall consider only the coupling to low-lying vibrational states. In what follows we will estimate (9.6) for the low-lying quadrupole vibration of ^{208}Pb.

Single-particle levels can be clearly identified in closed-shell nuclei. The nucleus $^{208}_{82}$Pb is a paradigm of such systems, the single-particle gap for neutrons ($N = 126$), i.e. the energy difference between the last occupied $3p_{1/2}$ orbital and the first empty state $2g_{9/2}$ is 3.1 MeV. Making use of equations (7.37) and (7.38) we obtain $\hbar\omega = 0.7$ MeV and $\beta_2 = 0.11$. An estimate for the radial matrix element derived in Appendix D is $\langle j|R_0 \partial U/\partial r|j\rangle \approx -50$ MeV. Substituting into

https://doi.org/10.1017/9781009401920.010 Published online by Cambridge University Press

equation (9.4) one obtains

$$V^2(\nu_1, \nu_1; \lambda = 2) = 0.6\,\mathrm{MeV}^2 \tag{9.7}$$

and

$$\Sigma^{\lambda=2}(\nu_1) = -0.9\,\mathrm{MeV}. \tag{9.8}$$

The estimate given in equation (9.8) is very sensitive to the parameters used. In particular a more realistic value of $\hbar\omega_2$ as well as of β_2 will reduce it considerably.

On the other hand the contribution of $\lambda = 4$ phonons and other j-values in the intermediate state would increase the estimate for the level shift. We retain the value $\Sigma(\nu_1) \approx -0.9\,\mathrm{MeV}$ for the purposes of the present section. The self-energy of a hole level has a similar magnitude but with opposite sign so the spacing between the occupied and unoccupied neutron levels would be reduced by 1.8 MeV. The ansatz that this reduction leads to the experimental value of 3.1 MW implies that the single-particle gap predicted by HF theory is 4.9 MeV (see Section 8.2). Because the density of levels is inversely proportional to the mass of the particle (see Appendix B) the above result corresponds to an effective mass (called ω-mass, see next section)

$$\frac{m^*}{m} \approx \frac{4.9}{3.1} = 1.6. \tag{9.9}$$

It could be argued that the relation $\mathrm{d}\varepsilon/\mathrm{d}k \sim 1/m^*$ was obtained for a uniform system. To bridge the gap between infinite nuclear matter and the case of potential wells of finite range let us consider a particle of mass m in a one-dimensional harmonic oscillator, which provides a sensible parametrization of the Saxon–Woods potential (see Fig. 9.3). It would be argued that in this case the density of levels is inversely proportional to the square root of the mass of the particle, in keeping with the fact that $\hbar\omega_0 = \hbar(C/m)^{1/2}$, C being the restoring force of the system. This is not the case as can be seen by writing the above relation in terms of the unit length parameter $b = (\hbar/m\omega_0)^{1/2}$, namely $\hbar\omega_0 = \hbar^2/mb^2$. Requiring the ground-state wavefunction $\Psi_0(r) \sim \exp(-r^2/2b^2)$ to have the same radial spread ($b = \text{const.}$) when one replaces the mass of the particle m by $m^* > m$, the density of levels turns out thus to be proportional to the effective mass, as in the infinite system discussed in Appendix B.

9.1.2 Motion of a particle in a complex potential

There is extensive experimental evidence showing that a nucleon moving in an orbital close to the Fermi energy has a mean free path which is large compared with the nuclear dimensions and it is effectively in a stationary state. Consequently the wavefunction can be written as $\varphi_1(\vec{r}, t) = \varphi_1(\vec{r})\mathrm{e}^{-\mathrm{i}\omega t}$. For single-particle levels progressively removed from the Fermi energy, the probability of finding states

https://doi.org/10.1017/9781009401920.010 Published online by Cambridge University Press

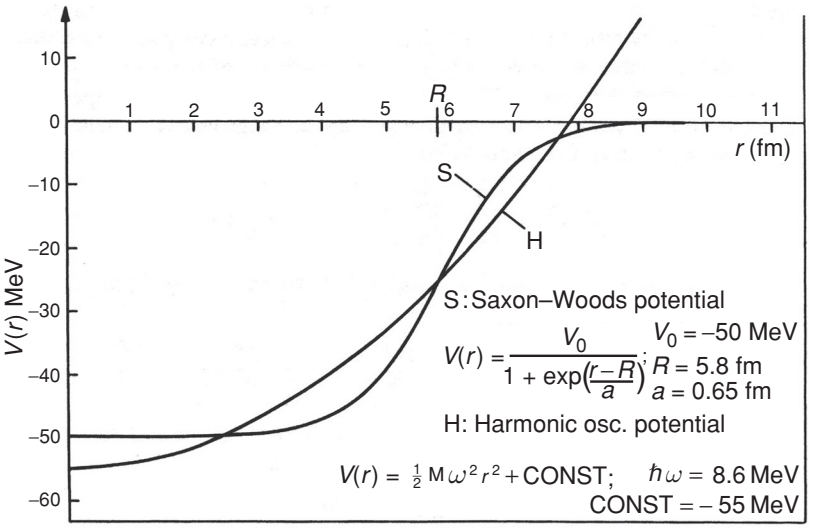

Figure 9.3. Comparison of a typical Saxon–Woods shell model potential and of a harmonic oscillator potential whose frequency has been chosen in order to fit the Saxon–Woods potential. (From Bohr and Mottelson (1969))

with the same energy as the single-particle state becomes sizable, in particular, states built out of a single particle and a collective surface vibration. Under these circumstances, the single-particle levels acquire a width and the associated wavefunction can be written as $\varphi_1(\vec{r}, t) = \varphi_1(\vec{r})\mathrm{e}^{-\mathrm{i}\omega t}\mathrm{e}^{-\frac{\Gamma}{2\hbar}t}$. Consequently, the probability of finding the state 1 occupied by a particle at time t, when it was occupied with probability 1 at time $t = 0$ decays exponentially with time, $\int \mathrm{d}^3r\ |\varphi_1(\vec{r}, t)|^2 = \exp^{-\frac{\Gamma}{\hbar}t}$. The associated lifetime of the state is connected to the width Γ by Heisenberg's uncertainty relation,

$$\tau = \frac{\hbar}{\Gamma}. \tag{9.10}$$

The width Γ is associated with the imaginary part of the self-energy of a particle. When the energy of the intermediate state $\varepsilon_2 + \hbar\omega_\lambda$ coincides with the energy ε_1 of the initial state the first term in the expression for the self-energy diverges. The divergence can be avoided by making an energy average, replacing ω by $\omega + \mathrm{i}\frac{I}{2}$, where I represents the energy interval over which averages are carried out. The self-energy operator can then be written as

$$\Sigma(1, \omega + \mathrm{i}I) = \Delta E(1, \omega + \mathrm{i}I) - \frac{\mathrm{i}}{2}\Gamma(1, \omega + \mathrm{i}I), \tag{9.11}$$

the sum of a real and an imaginary term. The final result, obtained by taking the limit of $\Sigma(1, \omega + \mathrm{i}I)$ as $I \to 0$, should not depend on the averaging process.

https://doi.org/10.1017/9781009401920.010 Published online by Cambridge University Press

It is illuminating to calculate the imaginary part of the self-energy, i.e.

$$\Gamma(1,\omega) = \sum_{2,\lambda} V^2(1,2;\lambda) \frac{I}{(\omega - (\varepsilon_2 + \omega_\lambda))^2 + (\frac{I}{2})^2}. \tag{9.12}$$

Taking the limit of this function as $I \to 0$ one obtains

$$\Gamma(1,\omega) = 2\pi \sum_{2,\lambda} V^2(1,2;\lambda)\delta(\omega - (\varepsilon_2 + \omega_\lambda)). \tag{9.13}$$

Approximating $V(1,2;\lambda)$ by its average value V leads to the formula

$$\Gamma(1,\omega) = 2\pi V^2 \varrho(\omega), \tag{9.14}$$

where the quantity $\varrho(\omega) = \sum_{2,\lambda} \delta(\omega - (\varepsilon_2 + \omega_\lambda))$ is the density of final states per unit energy, into which the particle state can decay. This is just the Golden Rule and is the basic expression used to describe the decay width of a quantal state. For scattering states, the quantity $-\frac{1}{2}\Gamma$ can be identified with the imaginary part of the optical potential.

A simple empirical parametrization of the damping width is provided by the relation (see Fig. 9.4)

$$\Gamma^{\downarrow}_{\rm sp} \approx 0.5\hbar\omega, \tag{9.15}$$

where $\hbar\omega$ is the single-particle energy measured from the Fermi energy ($\hbar\omega = |\varepsilon_1 - \varepsilon_{\rm F}|$). This parametrization is supported by detailed calculations: Bortignon

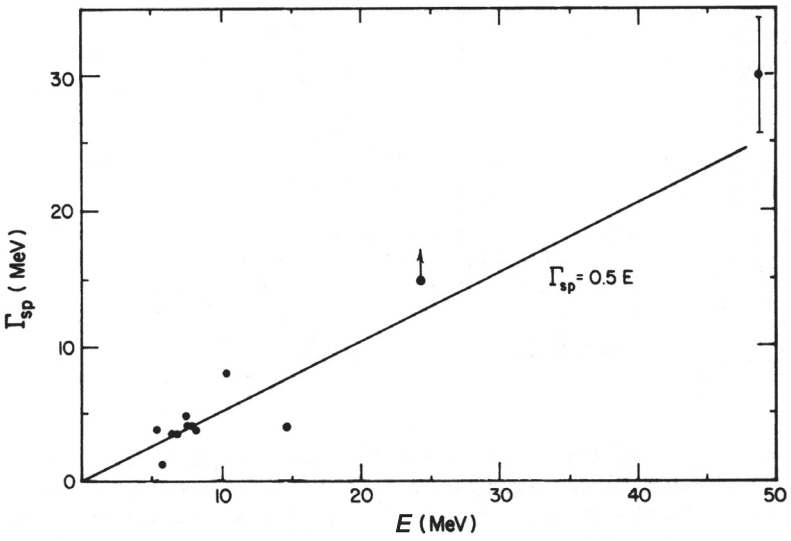

Figure 9.4. Full width at half maximum of the strength function associated with deep hole states, bound states and scattering states in a variety of nuclei. (From Bortignon *et al.* (1998))

https://doi.org/10.1017/9781009401920.010 Published online by Cambridge University Press

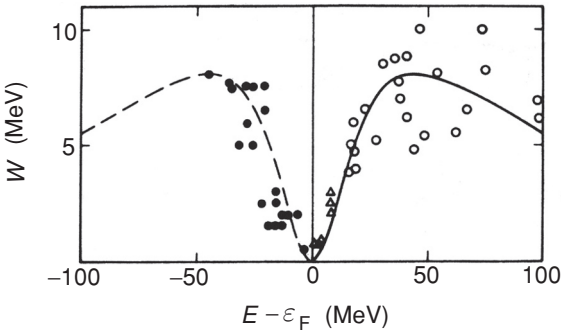

Figure 9.5. Dependence upon $\omega = E - \varepsilon_F$ of the imaginary part of the optical potential for nuclei with mass number $12 \leq A \leq 60$. (After Mahaux *et al.* (1985))

et al. (1986), Donati *et al.* (1996). Inserting the estimate given in equation (9.7) of the square of the particle-vibration coupling matrix elements and the empirical expression equation (9.15) into equation (9.14), we get an estimate for the density of intermediate states,

$$\varrho(\omega) = \frac{0.5\,\hbar\omega}{2\pi}\frac{}{V^2} \approx 0.13(\hbar\omega)\,\mathrm{MeV}, \tag{9.16}$$

where $\hbar\omega$ is the single-particle energy measured from the Fermi energy expressed in MeV. In order that the single-particle state $|\nu\rangle$ can undergo a real transition into states composed of a particle and a vibration, the density of states should be sufficiently large ($\varrho(\omega) \gtrsim 1\,\mathrm{MeV}^{-1}$). Thus damping will become important when $\hbar\omega \gtrsim 7$ MeV. On the other hand, for single-particle levels lying far away from the Fermi energy the virtual processes become unimportant and the effective mass of the nucleon coincides with the k-mass, while real processes give a damping width to these states (see Fig. 9.5).

9.2 Effective mass (ω-mass)

As the graphical perturbation expansion of the single-particle self-energy suggests (see Fig. 9.2 and equation (9.11)), the Hamiltonian describing the single-particle motion reads (see also equation (8.9)),

$$H_{\mathrm{s.p.}} = \left[-\frac{\hbar^2}{2m}\nabla^2 + \tilde{V}(k) + \Delta E(\omega) \right] + U(r) + \mathrm{i}W(\omega), \tag{9.17}$$

where $\Delta E(\omega)$ is the real part of the self-energy and $W = -\frac{1}{2}\Gamma$ is the imaginary part of the optical potential. The dependence of $\tilde{V}(k)$ on the momentum of the particle is associated with the non-locality arising from the Pauli principle, and has been discussed in Section 8.2.1. The dependence of $\Delta E(\omega)$ on the frequency is associated with the non-locality in time generated by the coupling to a surface

https://doi.org/10.1017/9781009401920.010 Published online by Cambridge University Press

vibration excited by the particle at a given time and reabsorbed at a different time (virtual, off the energy shell-processes). Effects associated with real, on the energy shell-processes are described by W(ω).

For many purposes it is possible to rewrite the term in square brackets in equation (9.17) as a kinetic energy term with an effective mass m^* (see e.g. Mahaux *et al*. (1985)). In fact, requiring that (in keeping with the fact that one is calculating an inertia, see Appendix B)

$$\frac{\mathrm{d}\hbar\omega}{\mathrm{d}k} = \frac{\hbar^2 k}{m^*},$$

and calculating

$$\frac{\mathrm{d}\hbar\omega}{\mathrm{d}k} = \frac{\hbar^2 k}{m} + \frac{\partial \tilde{V}(k)}{\partial k} + \frac{\partial \Delta E(\omega)}{\partial \hbar\omega}\frac{\mathrm{d}\hbar\omega}{\mathrm{d}k}, \tag{9.18}$$

which is equivalent to

$$\frac{\mathrm{d}\hbar\omega}{\mathrm{d}k} = \frac{\hbar^2 k}{m}(1 - \frac{\partial \Delta E}{\partial \omega})^{-1}(1 + \frac{m}{\hbar^2 k}\frac{\partial \tilde{V}(k)}{\partial k}), \tag{9.19}$$

one obtains

$$\frac{m^*}{m} = \frac{m_k}{m}\frac{m_\omega}{m}. \tag{9.20}$$

In this equation the ω- and k-masses are given by

$$\frac{m_\omega}{m} = (1 - \frac{\partial \Delta E(\omega)}{\partial \hbar\omega}), \qquad \frac{m_k}{m} = \left(1 + \frac{m}{\hbar^2 k}\frac{\partial \tilde{V}(k)}{\partial k}\right)^{-1}, \tag{9.21}$$

where the ω-derivative is to be calculated at the Fermi energy, while m_k/m coincides with the k-mass defined in Section 8.2.1. Consequently,

$$H_{\mathrm{s.p.}} = -\frac{\hbar^2}{2m^*}\nabla^2 + \tilde{U} + \mathrm{i}\widetilde{W}, \tag{9.22}$$

which is the optical-model Hamiltonian with $\tilde{U} = (m/m^*)U$ and $\widetilde{W} = (m/m^*)W$. Note that m^* can have a radial dependence ($m^*(r)$).

In Fig. 9.6 we display results of calculations of the ω-mass for the single-particle and single-hole states of ^{208}Pb (see also equation (9.9)). The quantity m_ω/m has a peak as a function of the single-particle energy centred around ε_{F}, such that

$$\frac{m^*}{m} = \frac{m_\omega}{m}\frac{m_k}{m} \approx 1.4 \times 0.7 \approx 1.$$

The associated FWHM is approximately 10 MeV, i.e. the ω-mass increase over the bare mass happens in the interval of energy between -5 MeV and $+5$ MeV

https://doi.org/10.1017/9781009401920.010 Published online by Cambridge University Press

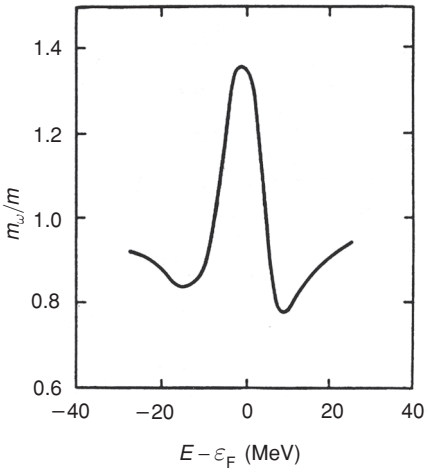

Figure 9.6. The ratio m_ω/m of the ω-mass of a nucleon in ^{208}Pb to the bare nucleon mass as a function of the energy of the particle measured with respect to the Fermi energy, calculated within the particle-vibration coupling model. (After Mahaux *et al*. (1985))

around the Fermi energy. This width is controlled by the frequency of collective surface vibrations which, in ^{208}Pb, correspond to an energy of the order of a few MeV. Consequently, for frequencies of the single particle much higher than this value, the phonons cannot dress the particle in an efficient way any more. Within the same interval of energy around the Fermi energy for which $m_\omega/m > 1$, the imaginary part of the self-energy (see Fig. 9.5 and equation (9.15)) is essentially zero. This is because no real transitions exist in this energy interval ($\varrho(\omega) < 1\,\mathrm{MeV}^{-1}$, see equation (9.16)). Furthermore, the result that the ω-mass is larger than the bare mass has the consequence that the density of levels around the Fermi energy is larger than that predicted by Hartree–Fock theory, in accordance with the experimental findings (see Fig. 8.8).

From these results one can understand why the empirical evidence concerning the energy of single-particle levels around the Fermi energy is well described by the motion of nucleons in a real, energy-independent, average potential, with a mass equal to the bare nucleon mass. However, there is a basic difference between this simple model and the results expressed by equation (9.17). In fact, in the empirical independent particle model the occupation of each level is either 1 or 0. The situation is more subtle here. Owing to its coupling to the nuclear surface, a particle which starts in a pure single-particle configuration is forced into more complicated states of motion. Consequently, the probability of finding a particle in a single-particle state below the Fermi level is different from 1. Similarly, unoccupied states at the level of the pure independent particle model become partially occupied as the particle jumps to these states by exciting a

https://doi.org/10.1017/9781009401920.010 Published online by Cambridge University Press

surface mode. In fact, the quantity

$$Z_\omega = (m_\omega/m)^{-1} \tag{9.23}$$

is the single-particle spectroscopic factor at the Fermi energy (quasiparticle strength, see Appendix E, equation (E.18)).

The fact that the 'more complicated' states to which the particle states couple can be at a higher energy than the original energy available to the particle presents no contradiction, as these are virtual states, i.e. states which last a finite amount of time (off the energy shell-processes). Because of Heisenberg's relations, energy does not need to be conserved within a range which becomes larger the shorter the time the intermediate state is virtually excited. However, an external field, such as that produced by a proton, can provide the necessary energy to make the process real and eventually pick up a neutron in the reaction $A(p, d)B$ from states above the Fermi energy. Results of calculations of the occupation number

$$n_j = \begin{cases} 1 + \frac{\mathrm{d}\Delta E'}{\mathrm{d}E} & j = \text{occ. orbit}, \\ -\frac{\mathrm{d}\Delta E'}{\mathrm{d}E} & j = \text{empty orbit} \end{cases} \tag{9.24}$$

are given in Fig. 9.7. In the above equation, the quantity $\Delta E'$ is the contribution associated with Fig. 9.2(b) arising from ground-state correlations.

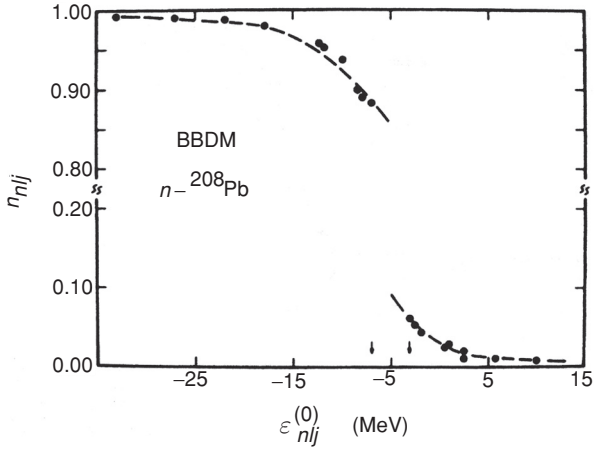

Figure 9.7. Occupation probability of neutron orbits in the correlated ^{208}Pb nucleus plotted against the single-particle energy ε_{nlj} computed in the Skyrme III-Hartree–Fock approximation. The calculation is based on equation (9.24). The dots correspond to the $1f_{7/2}$, $2p_{1/2}$, $1g_{7/2}$, $1h_{11/2}$, $1h_{9/2}$, $2f_{7/2}$,$2f_{5/2}$, $1i_{13/2}$, $3p_{3/2}$ and $3p_{1/2}$ hole states, and to the $2g_{9/2}$, $1i_{11/2}$, $1j_{15/2}$, $3d_{5/2}$, $2g_{7/2}$, $4s_{1/2}$, $3d_{3/2}$, $2h_{11/2}$ and $2h_{9/2}$ particle states. The dashed curve has been drawn to guide the eye through the calculated dots in order to exhibit their trend. The arrows show the location of $\varepsilon_{\mathrm{F}}^- = \varepsilon_{3p_{1/2}}$ and $\varepsilon_{\mathrm{F}}^+ = \varepsilon_{2g_{9/2}}$ (After Mahaux *et al.* (1985))

https://doi.org/10.1017/9781009401920.010 Published online by Cambridge University Press

The physics which is at the basis of the results displayed in Figs. 9.5 and 9.6 finds a compact expression in the dispersion relation (Mahaux *et al*. (1985))

$$\Delta E(\omega) \approx \frac{P}{\pi} \int \frac{W(\omega')}{\omega - \omega'} \mathrm{d}\omega'.$$

In this equation, P stands for the principal part integral for the real and imaginary parts of an analytic function (see equation (9.11)), i.e.

$$P \int_a^b f(x)/(x - x_0)\mathrm{d}x = \lim_{\delta \to 0^+} \left[\int_a^{x_0 - \delta} + \int_{x_0 + \delta}^b \right]$$

Because energy-conserving, on-the-energy shell processes are easier to calculate than virtual, off-the-energy shell processes, the dispersion relation above can be used in calculating the real potential from a known imaginary potential (see (9.17)).

9.3 The ω-mass and the induced interaction

In this section we obtain an expression for the ω-mass in a simplified version of the particle-vibration coupling model and show how it is related to the induced pairing interaction between nucleons resulting from the exchange of surface phonons. The self-energy of a nucleon is due to the emission and absorption of a virtual phonon as illustrated in Fig. 9.2 while the induced interaction is represented by Fig. 8.3(c). The general particle-vibration coupling model is simplified by considering coupling with only one type of phonon with frequency ω_λ and by assuming that the single nucleon levels are uniformly distributed around the Fermi level. A more systematic discussion of the induced nucleon–nucleon interaction due to phonon exchange will be presented in the next chapter.

The single-particle self-energy expression given in equation (9.1) is the sum of a polarization term $\Sigma^{(\mathrm{p})}(\omega)$ (Fig. 9.2(a)) and a core correlation term $\Sigma^{(\mathrm{c})}(\omega)$ (Fig. 9.2(b)) They give equal contributions to the ω-mass at the Fermi level in the simplified model considered here. The polarization term is

$$\Sigma_\nu^{(\mathrm{p})}(\omega) = \Delta E^{(\mathrm{p})}(\omega) = \sum_{\nu'} \frac{V^2(\nu, \nu'; \lambda)}{\omega - (e_{\nu'} + \hbar\omega_\lambda)}, \tag{9.25}$$

where $e_{\nu'} = \varepsilon_{\nu'} - \varepsilon_{\mathrm{F}}$ and $\omega = e_\nu - \varepsilon_{\mathrm{F}}$. At the Fermi energy $\omega = 0$ and

$$\begin{aligned} \left. \frac{\partial \Delta E_\nu^{(\mathrm{p})}(\omega)}{\partial \omega} \right|_{\omega=0} &= -\sum_{\nu'} \left. \frac{V^2(\nu, \nu'; \lambda)}{(\omega - (e_{\nu'} + \hbar\omega_\lambda))^2} \right|_{\omega=0} \\ &= -\sum_{\nu'} \frac{V^2(\nu, \nu'; \lambda)}{(e_{\nu'} + \hbar\omega_\lambda)^2}. \end{aligned} \tag{9.26}$$

https://doi.org/10.1017/9781009401920.010 Published online by Cambridge University Press

If the sum is approximated by an integral assuming a density of single-particle states of one-spin orientation at the Fermi level $N(0)$ ($g/2$ in equation (3.58), $1/d$ and $3A/8E_F$ in equation (2.1)) and constant single-particle matrix elements V we get

$$\left.\frac{\partial \Delta E_\nu^{(p)}(\omega)}{\partial \omega}\right| \approx -N(0)\int_0^\infty \frac{V^2 \mathrm{d}e}{(e+\hbar\omega_\lambda)^2} = -N(0)\frac{V^2}{\hbar\omega_\lambda}. \tag{9.27}$$

The core correlation part of the self-energy gives an equal contribution so that the total value is

$$\left.\frac{\partial \Delta E_\nu(\omega)}{\partial \omega}\right| = -2N(0)\frac{V^2}{\hbar\omega_\lambda}. \tag{9.28}$$

Consequently the ω-mass defined in equation (9.21) is

$$m_\omega = m\left(1 - \frac{\partial \Delta E_\nu^{(p)}(\omega)}{\partial \omega}\right) = m(1+\lambda_{\text{p-v}}). \tag{9.29}$$

The quantity $\lambda_{\text{p-v}}$ is defined by

$$\lambda_{\text{p-v}} = N(0)\frac{2V^2}{\hbar\omega_\lambda} = N(0)g_{\text{p-v}}, \tag{9.30}$$

where

$$g_{\text{p-v}} = \frac{2V^2}{\hbar\omega_\lambda}, \tag{9.31}$$

is a particle-vibration coupling parameter. The factor $(1+\lambda_{\text{p-v}})$ is known as the mass enhancement factor.

The vibration excited by a nucleon interacting with the surface can be absorbed by a second nucleon as shown in Fig. 8.3(c), giving rise to an induced interaction. In this section we are interested in the induced interaction which contributes to pairing. Nucleons in time-reversed states $|\nu\rangle$ and $|\bar{\nu}\rangle$ with energies ε exchange a phonon and make a transition to final states $|\nu'\rangle$ and $|\bar{\nu}'\rangle$ with energies ε' as illustrated in the inset of Fig. 10.1. The transition matrix element is

$$v_{\nu\nu'} = \frac{2V^2(\nu,\nu';\lambda)}{\varepsilon_\nu - (\varepsilon_{\nu'}+\hbar\omega_\lambda)}. \tag{9.32}$$

The factor 2 arises because there are two possible processes each giving the same matrix element: the phonon may be emitted by the state $|\nu\rangle$ and absorbed by $|\bar{\nu}\rangle$, and vice versa. The matrix element is not symmetric in the initial and final state.

https://doi.org/10.1017/9781009401920.010 Published online by Cambridge University Press

A symmetrized form can be obtained by interchanging the initial and final states and averaging

$$v_{\nu\nu'} = \frac{V^2(\nu, \nu'; \lambda)}{\varepsilon_\nu - (\varepsilon_{\nu'} + \hbar\omega_\lambda)} + \frac{V^2(\nu, \nu'; \lambda)}{\varepsilon_{\nu'} - (\varepsilon_\nu + \hbar\omega_\lambda)} \tag{9.33}$$

$$= \frac{2\hbar\omega_\lambda V^2(\nu, \nu'; \lambda)}{(\varepsilon_\nu - \varepsilon_{\nu'})^2 - (\hbar\omega_\lambda)^2}. \tag{9.34}$$

For $\varepsilon_\nu \approx \varepsilon_{\nu'} \approx \varepsilon_{\mathrm{F}}$ and assuming a constant particle-vibration coupling matrix elements V, one obtains

$$v_{\nu\nu'} = -\frac{2V^2}{\hbar\omega_\lambda} = -g_{\text{p-v}}. \tag{9.35}$$

Making use of typical values of $\lambda_{\text{p-v}} \approx 0.6$ (see equation (9.9) and Fig. 9.6) and $N(0) \approx 3.4\,\mathrm{MeV}^{-1}$ (e.g. ^{120}Sn, see Fig. 8.4 and discussion following (8.21)) one obtains from equations (9.30) and (9.35) $\bar{v} = -0.2\,\mathrm{MeV}$ (see also Section 10.2, discussion in paragraph before equation (10.20)).

The bare nucleon–nucleon interaction is essential for the production of pair correlations in nuclei, but the induced interaction due to phonon exchange also contributes. In order to assess the importance of the induced interaction we make an estimate of the pairing gap, neglecting the bare interaction completely. The pairing gap equation with the interaction $v_{\nu\nu'} = -g_{\text{p-v}}$ is

$$\Delta = g_{\text{p-v}} \sum_{\nu>0} \frac{\Delta}{2E_\nu}. \tag{9.36}$$

By approximating the sum by an integral this relation can be written as

$$1 = g_{\text{p-v}} N(0) \int_{-\omega_D}^{\omega_D} \mathrm{d}e \frac{1}{\sqrt{e^2 + \Delta^2}} \approx g_{\text{p-v}} N(0) \sinh^{-1}\left(\frac{\omega_D}{\Delta}\right), \tag{9.37}$$

where $N(0)$ is the density of levels at the Fermi energy for one-spin orientation, and ω_D is a typical energy associated with surface vibrations. From the relation above one obtains

$$\Delta = \omega_D \left(\sinh\left(\frac{1}{\lambda_{\text{p-v}}}\right)\right)^{-1}. \tag{9.38}$$

In the case in which $\lambda_{\text{p-v}} \ll 1$ (weak coupling limit) one can write (see (3.58))

$$\Delta = 2\omega_D \exp\left(-\frac{1}{\lambda_{\text{p-v}}}\right), \tag{9.39}$$

while

$$\Delta = \omega_D \lambda_{\text{p-v}} \tag{9.40}$$

https://doi.org/10.1017/9781009401920.010 Published online by Cambridge University Press

in the case in which $\lambda_{\text{p-v}} \gg 1$ (strong coupling limit).

Making use of typical values of $\lambda_{\text{p-v}} \approx 0.6$ (see (9.9)) and $\omega_D \approx 1$–2 MeV, one expects from equation (9.39) the induced interaction arising from the exchange of low-lying collective surface vibrational states to give rise to pairing gaps of the order of 0.4–0.8 MeV, i.e. pairing gaps which are of the order of 50% of the empirical value $12/\sqrt{A}$ MeV.

The above treatment of the consequences the fermion–boson (particle–vibration) coupling has on the properties of the single-particle states neglects two major effects (see Sections 9.1 and 9.2, see also Schrieffer (1964) equation (7.83); note that $Z(p_\Delta)$ is the inverse of Z_ω). Firstly, the single-particle strength is reduced from the value of 1 to a smaller value Z_ω (see equation (9.23)). Secondly, the single-particle states acquire a finite width $\Gamma(\omega)$. These effects can change quantitatively the estimates given in Equations (9.39) and (9.40). In particular, considering only the effect of the width, i.e. setting $Z_\omega = 1$, Morel and Nozières (1962) found, for the case of an infinite system,

$$\Delta(\vec{k}) = \int V\left(\vec{k} - \vec{k}'\right) \frac{\Delta(k')}{2E_{k'}} \left[\frac{2}{\pi} \tanh^{-1}\left(\frac{E_{k'}}{\Gamma_{k'}}\right)\right] \frac{\mathrm{d}^3k'}{(2\pi)^3} \tag{9.41}$$

where $\vec{k}$ is the momentum of the single particle and $V(\vec{k} - \vec{k}')$ is the (state dependent) two-body interaction. The effect of the bracketed factor is to cut off the integral when the imaginary part Γ_k reaches the same magnitude as E_k, thus reducing the prefactor appearing in equations (9.39) and (9.40) (see also Baldo *et al*. (2002)).

The fact that there is an explicit relation between the value of the induced pairing interaction, of the ω-mass, of the occupation number Z_ω and of the damping width $\Gamma(\omega)$ is closely connected to sum rule arguments (Ward identities) relating self-energy and vertex correction processes to particle conservation (see Section 8.3.4 and Fig. 8.16) (see also Mahan (1981)).

Note that one has also neglected some of these relations and effects when discussing the results displayed in Fig. 8.6 and 8.9. They are taken up in Section 10.4, in connection with the results displayed in Fig. 10.16 (see also Appendix H, Section H.4, as well as Terasaki *et al*. (2002a, 2002b)).

Let us close this section by relating equation (9.40) to the single j-shell equation (H.30). Because $N(0) = \sum_j \Omega_j/2\omega_D = \Omega/2\omega_D$, where $\Omega_j = (2j+1)/2$, equation (9.40) can also be written as

$$\Delta = \frac{1}{2} g_{\text{p-v}} \Omega. \tag{9.42}$$

https://doi.org/10.1017/9781009401920.010 Published online by Cambridge University Press